# Stark-induced $L$-mixing interferences in ultracold cesium Rydberg atoms

Hao Zhang, Limei Wang, Linjie Zhang, Changyong Li, Liantuan Xiao, Jianming Zhao,* and Suotang Jia
*State Key Laboratory of Quantum Optics and Quantum Optics Devices, Laser Spectroscopy Laboratory, Shanxi University, Taiyuan 030006, P.R. China*

Patrick Cheinet, Daniel Comparat, and Pierre Pillet
*Laboratoire Aimé Cotton, CNRS, Université Paris-Sud, ENS Cachan, Bâtiment 505, 91405 Orsay, France*
(Received 22 October 2012; published 5 March 2013)

The $l$-mixing effect and state-transfer induced by an external electric field pulse in ultracold Rydberg gases are observed with cesium atoms excited to $nS$ states, and measured with a state selective field ionization technique. High-$l$ states are populated from the initially excited $nS$ states due to non-adiabatic transitions through avoided crossings that are formed between the $nS$ state and the $(n-4)$ manifold. The population of the product state is investigated as a function of the electric field pulse parameters. The coherent property of the transfer is demonstrated using a 2-pulse sequence and the results are consistent with the theoretical calculations. This $l$-mixing phenomenon in the electric field may be used to help forming a molecular potential and create Rydberg molecules.

DOI: 10.1103/PhysRevA.87.033405 PACS number(s): 32.80.Ee, 32.80.Xx

Ultracold Rydberg atoms have generated considerable interest in recent decades because of their long lifetimes and strong long-range dipole-dipole interactions. Additionally, their collective, many-body properties make them promising candidates to implement quantum gates [1–4] and realize single-photon sources [5]. Cold Rydberg atoms provide a collision-rich environment which has revealed spontaneous evolution to cold plasmas [6,7] and $l$ mixing due to interaction between electrons or ions and the cold Rydberg atoms [8,9].

Rydberg states are extremely sensitive to external electric fields, due to their large polarizability, which scales as $n^7$. The electric field can be used to precisely tune energy levels and further increase the interaction strength between Rydberg atoms using a Förster resonance [10,11]. The behavior of resonant dipole-dipole interactions of Rydberg states has been addressed both theoretically and experimentally [12]. An important effect of the electric field is $n$ mixing or $l$ mixing of Rydberg states with their nearby manifolds. $L$-mixing dynamics of Rydberg states of hydrogen atoms in a static electric field has been studied previously using exact analytical forms of the time-dependent Schrödinger equation [13]. Exact solutions of time-dependent equations have been obtained for the full array of angular momentum mixing transitions $nl$-$nl'$ in atomic hydrogen induced by collisions with charged particles [14]. The $l$ mixing in a sodium beam of Rydberg atoms caused by slow ion impact has been investigated experimentally [9], and the high-$l$ states' redistribution strongly depends on the impact velocity of the ions or electrons. The spontaneous evolution of cold Rydberg atoms from initially excited low-$l$ Rydberg states into long-lived, high-$l$ states [8] has been investigated in ultracold atom clouds, where $l$ change was mainly due to the collisions between slow free electrons and initially excited Rydberg atoms. On the other hand, pulsed electric fields have been used to control the atom-light interaction [15] and to populate the high-$l$ state in the Ba $6Pnl$ $(l > 4)$ state [16].

In this work, we report on the experimental observation and theoretical study of an electric-field-induced $l$-mixing population in a high-$l$ state from atoms originally excited in an $nS$ Rydberg state. The $nS$ states nonadiabatically transfer to high-$l$ states and form the product state in an applied electric-field pulse. A second electric-field pulse is used to investigate the coherence of this transfer. We first show the transfer and prove that the product state corresponds to high-$l$ states before extending the study of this effect.

The experimental setup consists of a standard cesium magneto-optical trap (MOT), with trapped atoms possessing a temperature of $\sim$100 $\mu$K and a peak density of $\sim 10^9$ cm$^{-3}$. There are two nonmagnetic grids located around the MOT, which are separated by 15 mm; one is used to apply a weak dc electric field to compensate a parallel stray field and the electric-field pulse applied to investigate the $l$ mixing; meanwhile, the second is used to apply a final ionizing field ramp. The electric field is calibrated by measuring the Stark splitting of $nD_{3/2,5/2}$ $(n = 60)$ state. The residual perpendicular field is estimated to be lower than 0.1 V/cm. The trapped atoms are excited to $nS$ Rydberg states using a two-photon transition, $6S \rightarrow 6P \rightarrow nS$. The first transition, accomplished by the trapping light, is tuned to resonance with the $6S_{1/2}$ $(F = 4) \rightarrow 6P_{3/2}$ $(F' = 5)$ transition. The laser light for the $6P \rightarrow nS$ transition (around 510 nm) is obtained by frequency doubling an amplified infrared diode laser. It is chopped into 500-ns pulses by an acousto-optical modulator and focused on the atomic sample, yielding a cylindrical excitation volume $\sim$800 $\mu$m long and $\sim$150 $\mu$m in diameter. The typical time sequence of the experiment is as follows: starting with a loaded MOT, the Rydberg excitation laser is turned on for 500 ns. This excitation is followed by an electric-field pulse with rise and fall times of typically 10 ns and with tunable duration from 30 ns to a few microseconds. Then the ionization ramp rises to its maximum value in 3 $\mu$s, which realizes a state-selective field ionization, enabling identification of different Rydberg states

*Corresponding author: zhaojm@sxu.edu.cn

 

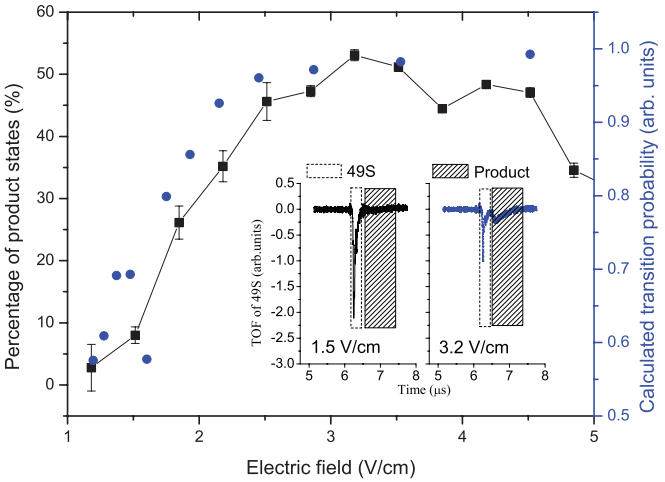


FIG. 1. (Color online) Inset: TOF spectra of the 49*S* state at an electric-field pulse of 1 $\mu$s and a strength of 3.2 V/cm (right) and 1.5 V/cm (left). The boxed and shaded area denote the position of 49*S*- and product-state atoms, respectively. Percentage of product-state over initially excited atoms, measured [(black) squares] and calculated [(blue) circles] as a function of the value of the electric-field pulse (see text).

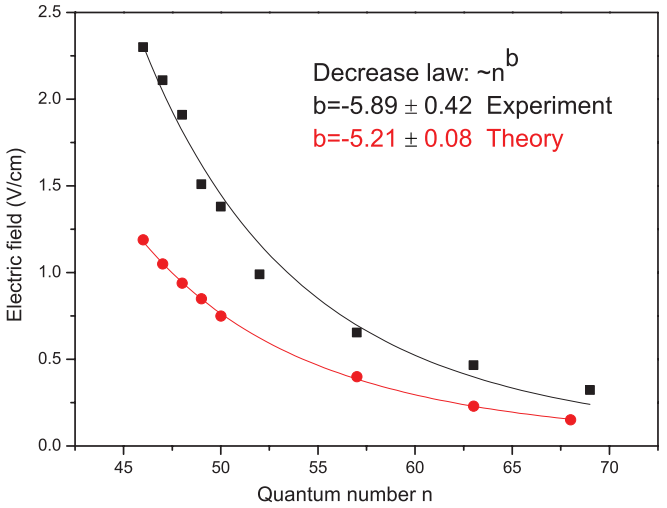


FIG. 2. (Color online) Calculated first avoided crossing points between *nS* and $(n-4)$ manifolds (red circles), and measured electric fields corresponding to product state percentage of 10% (black squares) versus principal quantum number n.

from the time-resolved ion spectrum or time of flight (TOF) before detection on a calibrated microchannel plate. Typically we excite several thousand *nS* atoms with a peak density of $\sim 10^8$ cm$^{-3}$. The insets in Fig. 1 show the TOF signal for $n = 49$ recorded for two strengths of the applied electric pulse of 1 $\mu$s. When applying a relatively weak electric-field pulse, it displays the 49*S* spectrum only.

The signal at a higher field strength clearly displays a new component, denoted by the shaded area in the insets in Fig. 1, which we call the product state, which possesses a higher ionization threshold. Figure 1 presents the obtained percentage of this product state as a function of the electric field strength. It should be noted that the efficiency of this transfer quickly increases above 50%. Figure 1 also presents a prediction (discussed later) which assumes a transfer to high-*l* states. The population in the product state strongly depends on the amplitude of the applied electric field pulse and begins developing at the electric field required to merge the *nS* Rydberg state into the $(n-4)$ manifold. As such, we attempt to demonstrate that the product corresponds to high-*l* states from this manifold. We first measure the required electric field to observe a 10% transfer to the product state as a function of the principal quantum number *n* (Fig. 2) together with the electric field corresponding to the first avoided crossing between the *nS* state and the manifold. As the principal quantum number increases, the field of the first avoided crossing decreases with the theoretical $n^{-5.21}$ law. The measured field is about 2 times larger than the first crossing field. Indeed, the arbitrarily chosen field displaying a 10% transfer rate cannot correspond to the first avoided crossing field, as the Stark mixing of the *nS* state with the manifold is still extremely small and this crossing should be traversed with a much smaller transfer. Nevertheless, we have shown that to observe the product state, the electric field needs to be sufficient to merge the *nS* state within the nearby manifold.

We now want to prove that the product state corresponds to high-*l* states. The two-photon excitation scheme we use can excite both *nS* and *nD* components. When applying a strong electric field, the Stark effect will mix a small component of the closest *nS* and *nD* states in the eigenstates of the manifold, allowing direct excitation. We zoom in on an avoided crossing point in the vicinity of 5.5 V/cm. In this specific measurement, the electric field is not pulsed but is constantly applied, while we keep all other parameters fixed. We then tune the 510-nm laser frequency to be able to excite atoms to 49*S* and directly to the high-*l* states. We display in Fig. 3(b) the left four excitation points, denoted A, B, C, and D, corresponding to the excitation of the Stark map calculated according to Ref. [17]. At points C and D, the Stark state is the equiprobable superposition of the *nS* and one high-*l* state and we observe both in the TOF, [Fig. 3(b)]. The resonance points A and B include instead a small fraction of the *nS* state and, thus, only display the TOF of the high-*l* states which possess a different ionization threshold compared to the *nS* state, appearing at the position of the product state. We conclude that the product state is a high-*l* state from the $(n-4)$ manifold. High-*l* states ionize with the scaling law $1/9n^4$ instead of the $1/16n^4$ for low-*l* states. This also explains why the observed ionization threshold is so different.

Now that we have identified the product state as a high-*l* state from the manifold, we want to study the physical effects causing the transfer. The strong interactions between Rydberg atoms could be the cause for this transfer, but we do not expect it because of the low Rydberg density in the experiment. To verify this, we performed a set of measurements for various densities by varying the 510-nm laser power. Figure 4 displays the number of atoms in product state as a function of the total Rydberg number at a field of $\sim$3.0 V/cm and different pulse durations. We do not observe the quadratic law that should occur for an interaction-induced transfer, but rather, the data are compatible with an approximate linear dependence. With very short pulses, which display a smaller

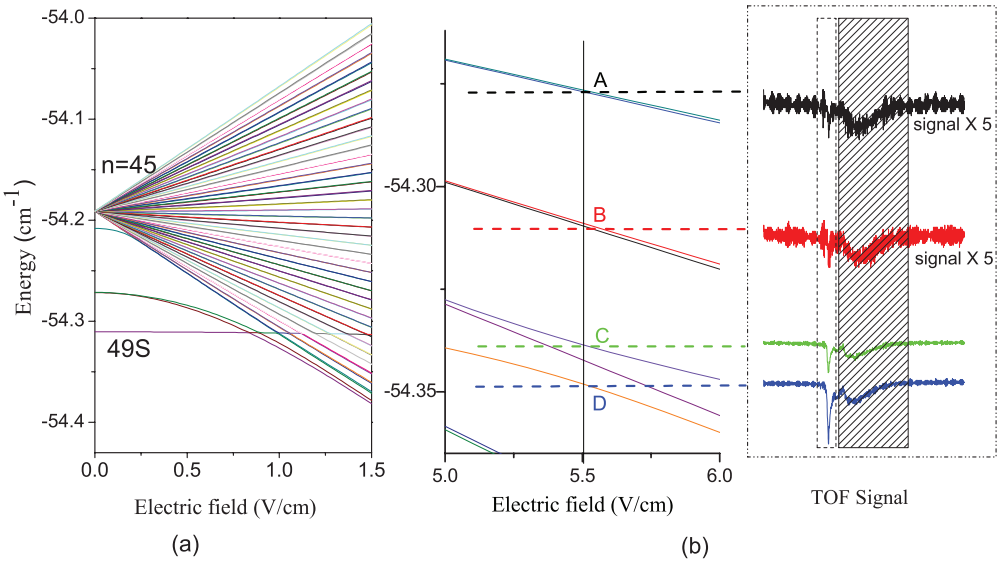


FIG. 3. (Color online) (a) Stark map in the vicinity of $n = 49S$ and $n = 45$ manifolds with $|m_j| = 1/2$. (b) TOF signals (right) and corresponding energies structure (left) (the top two curves are 5 times the origin signals). Dashed horizontal lines denote the resonant positions of high-$l$ states and avoided crossing at a dc field of 5.5 V/cm. Boxed and shaded areas are the same as in Fig. 1.

unsaturated transfer, we check that the linear dependence is not a consequence of saturated interactions. This constitutes proof that the effect involves a single Rydberg atom only. These results also imply that the transfer is not complete for any pulse length but develops over the electric field hold time. However, electric-field-induced dipole interactions would modify this single Rydberg Stark effect, and the process of transfer to a high-$l$ state includes part of a nonlinear interaction, leading to the deviation between the experimental data and the linear fittings.

We explain the observed transfer with multiple diabatic couplings at each avoided crossing between the $nS$ state and the manifold [shown in Fig. 3(a)], first during the switching-on, then during the switching-off of the electric field pulse. This leads to effective $l$ mixing. In cesium, the fractional quantum defect is small, leaving the $nS$ state close to the $(n-4)$ manifold, within which the $nS$ state merges for relatively low electric field strengths. For $n = 49$ this first contact occurs near 1 V/cm [see Fig. 3(a)]. This explains why the product state appears only after such a crossing field (see Fig. 1). As explained above, the external electric field is turned on with a finite rise time of $t = 10$ ns. The frequency energy gap $\Delta\nu$ at the avoided crossing depends strongly on the level crossing and increases for greater electric fields. The border between diabatic and adiabatic passage is reached when $t \sim 1/\Delta\nu$. For instance, this border is nearly reached for 3.4 V/cm for $n = 49$, where $\Delta\nu = 66$ MHz $\approx 1/(10$ ns). For fields higher than 3.4 V/cm, the avoided crossings become too large and the transfers between the $nS$ states and the manifold stop. This clearly explains why the product state saturates (Fig. 1). Due to the numerous crossings, the product-state amplitude will depend on the exact succession of couplings and should display fluctuations. Calculating these fluctuations is beyond the scope of this study, but we can use an approximation to estimate the initial increase. One can use a two-state theory to formulate a multilevel crossing problem if avoided crossing points are well separated from each other [18]. The probability of nonadiabatic transition at an avoided crossing point is given by

$$P = \exp\left(-2\pi \frac{(V_{ij})^2}{\hbar(dW/dt)}\right), \tag{1}$$

where $V_{ij}$ is the coupling between two Stark states at the avoided crossing point:

$$V_{ij} = \left\langle \Psi_i^{(S)} \middle| e\vec{r} \cdot \vec{E} \middle| \Psi_j^{(S)} \right\rangle \tag{2}$$

and

$$\Psi_k^{(S)} = \sum_n \sum_{l=|m|}^{n-1} \alpha_{n,l}^{n_1,n_2}(E)\phi_{nlm} \tag{3}$$

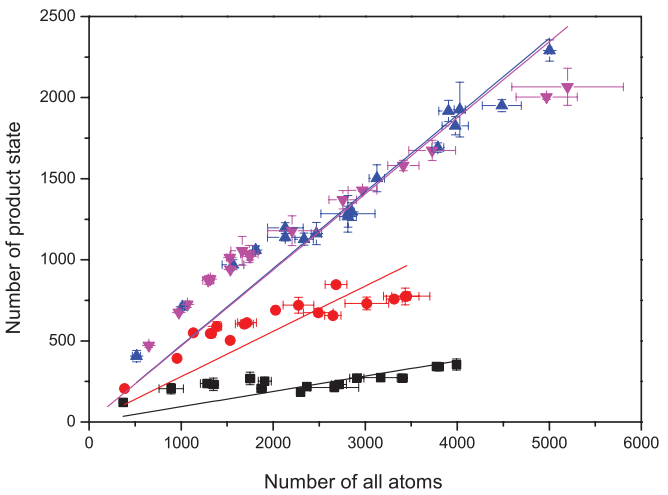


FIG. 4. (Color online) Measured number of atoms in product state as a function of initially excited atoms with an electric field of 3.0 V/cm and different electric pulse durations: 30 ns [(black) squares], 50 ns [(red) circles], 200 ns [upward (blue) triangles], and 500 ns [downward (pink) triangles]. Solid lines represent linear fits of the data.

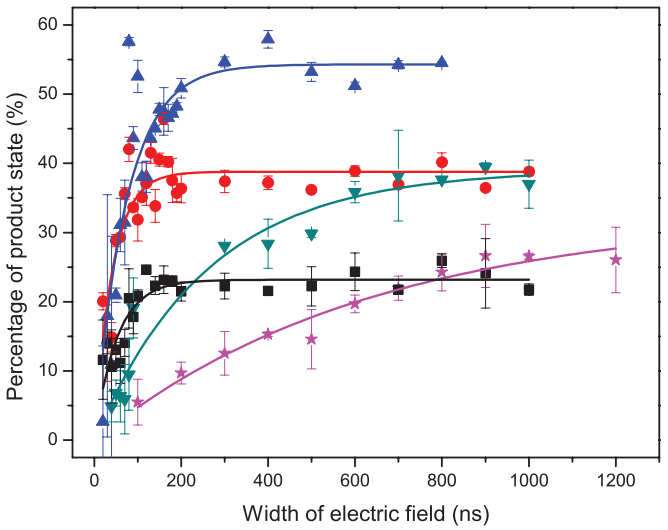


FIG. 5. (Color online) Percentage product state as a function of electric field duration for a field amplitude of 5.5 V/cm [(black) squares], 4.0 V/cm [(red) circles], 3.0 V/cm (upward triangles), 2.2 V/cm (downward triangles), and 1.5 V/cm [(pink) stars].

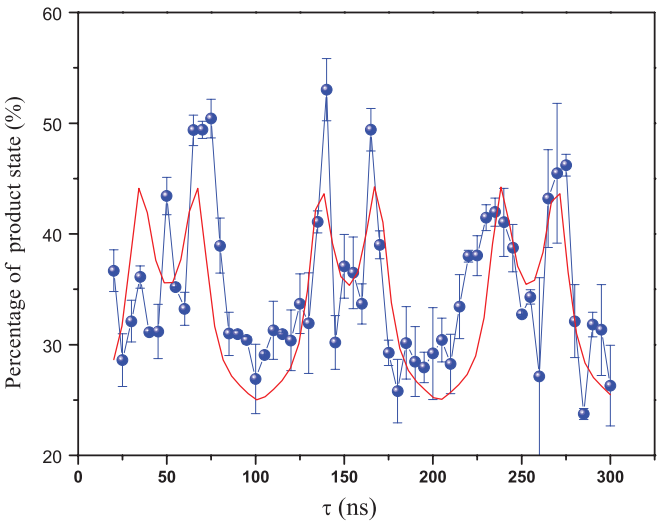


FIG. 6. (Color online) Transfer percentage as a function of $\tau$ between two electric field pulses with a field duration of 30 ns and an amplitude of 3.0 V/cm. The solid (red) line is the fit to the data with Eq. (4).

$\Psi_k^{(S)}$ is the Stark-state wave function, $\alpha$ is the element of the unitary matrix that projects the Stark states, labeled by the parabolic quantum numbers $n_1$ and $n_2$. $W$ is the energy of the Stark state, the slew rate is expressed as $dW/dt = (dW/dE)(dE/dt)$, and $dE/dt$ is the changing speed of the external electric field, here $dW/dE = 3(n_1 - n_2)n/2$.

According to Eq. (1), we calculate the nonadiabatic transition probabilities at the avoided crossing points and then sum them incoherently. The result is shown in Fig. 1 and is consistent with the experimental data.

As noted before, the transfer also depends on the hold time of the electric field pulse. Figure 5 shows the time evolution for different field strengths and a guide for the eye with an exponential law. It is not predictable with our previous model because it neglects coherence between the various populated states when the electric field is switched off. Indeed, after the field has been switched on, the system becomes a composite of the $nS$ state and manifold states with a well-defined phase. If no dephasing is accumulated, it will evolve back perfectly into the original $nS$ state. The time evolution would then come from the accumulated dephasing between the different populated states at the end of the electric field pulse. We have tested that no time evolution is visible, and only a very small fraction of the atoms end in the manifold when the electric field is already established during the Rydberg excitation or if we do not wait for the switch-off before applying the state-selective field ionization ramp. The evolution stops when the dephasing is so large that coherence is lost. The transfer could display oscillatory behavior if the dephasing of different populations is small enough and we can indeed guess some oscillations at the early times of the evolution of most curves in Fig. 5.

To better observe the interferences, we first use an electric field pulse which is short enough that some coherence remains in the superposition state. A second pulse with the same duration is applied after a variable hold time $\tau$ under zero field. During this hold time, all manifold states are then degenerate and only the $nS$ state dephases compared to them, leading to interference fringes with a good coherence time. Figure 6 shows the percentage of the product state with pulse durations of 30 ns at 3.0 V/cm and variable intermediate hold times $\tau$. We can clearly see oscillation of the product state and there are two peaks in each wave packet. At this electric field, the $nS$ state crosses about 10 other manifold states, which contribute to the product state, and the fringes are too complicated to simulate accurately. Nevertheless, we can use a simplified multilevel interference formula [19] to fit the experimental data in Fig. 6:

$$f(t) = A + \frac{a \sin^2 bt}{1 + c \sin^2 dt}, \tag{4}$$

in which $a$, $b$, $c$, and $d$ are fitting parameters. Here $a$ represents the amplitude of the wave packet and $c$ influences the internal amplitude structure of a single packet. $b$ and $d$ are the phase factors linked with the number of levels involved in the interferences. $A$ is the offset and is dependent on the amplitude and width of the electric pulse. Taking $d = 3b$ enables the fit of our data presented in Fig. 6, which suggests that only three levels from the manifold participate significantly in the interference for an electric field pulse amplitude of 3.0 V/cm and a duration of 30 ns.

The present study has demonstrated a transfer from an $nS$ state to a high-$l$ state in cesium due to partially coherent nonadiabatic transitions, but some of the characteristics remain difficult to explain. In Fig. 5, for example, the evolution time scale changes quickly from about $T = 1$ $\mu$s at 1.5 V/cm to $T = 100$ ns at 3.0 V/cm, but we would have expected a $T \sim 1/\Delta\nu$ type of law, that is, the time scale should be inversely proportional to the Stark splitting. In addition, the Stark splitting is of the order of 100 MHz for the Fig. 5 data such that we expect a much faster evolution, of the order of 10 ns. One possible explanation is that other $m$ (magnetic quantum number projection on the electric field axis) states are coupled rather than only the $|m_j| = 1/2$ states. However, we

have checked that switching off the MOT magnetic field did not noticeably change our results. Another possible explanation is that the coupling could originate from interactions, while the transfer itself is linear with the initial density because it comes from diabatic passages.

In conclusion, we have observed a state transfer from an initially excited $nS$ state to high-$l$ states induced by nonadiabatic transitions through avoided crossings between the $nS$ state and the $(n-4)$ manifold. The state transfer rate is strongly dependent on the applied electric field. As the applied field increases, so does the total transfer fraction from the $nS$ to higher-$l$ states, reaching efficiencies of $>50\%$. The time evolution of this transfer seems to be governed by interference effects between the different populated states. When fully understood, this phenomenon may be used to populate specific high-$l$ Rydberg states. This $l$-mixing phenomenon in the electric field may be used to form a potential [20] and create Rydberg molecules.

We appreciate fruitful discussions with C. L. Vaillant, A. McCulloch, and T. Vogt and thank Z. Feng for the initial experimental work. This work was supported by 973 (Grant No. 2012CB921603), the NSFC Project for Excellent Research Team (Grant No. 61121064), the Sino-French International Research Network on Quantum Manipulation of Atoms and Photons, and the National Natural Science Foundation of China (Grants No. 61078001, No. 11274209, No. 10934004, and No. 60978001).

[1] M. Saffman, T. G. Walker, and K. Mølmer, Rev. Mod. Phys. **82**, 2313 (2010).
[2] D. Jaksch, J. I. Cirac, P. Zoller, S. L. Rolston, R. Côté, and M. D. Lukin, Phys. Rev. Lett. **85**, 2208 (2000).
[3] M. D. Lukin, M. Fleischhauer, R. Côté, L. M. Duan, D. Jaksch, J. I. Cirac, and P. Zoller, Phys. Rev. Lett. **87**, 037901 (2001).
[4] L. Isenhower, E. Urban, X. L. Zhang, A. T. Gill, T. Henage, T. A. Johnson, T. G. Walker, and M. Saffman, Phys. Rev. Lett. **104**, 010503 (2010).
[5] Y. O. Dudin and A. Kuzmich, Science **336**, 887 (2012).
[6] M. P. Robinson, B. Laburthe Tolra, M. W. Noel, T. F. Gallagher, and P. Pillet, Phys. Rev. Lett. **85**, 4466 (2000).
[7] T. C. Killian, M. J. Lim, S. Kulin, R. Dumke, S. D. Bergeson, and S. L. Rolston, Phys. Rev. Lett. **86**, 3759 (2001).
[8] S. K. Dutta, D. Feldbaum, A. Walz-Flannigan, J. R. Guest, and G. Raithel, Phys. Rev. Lett. **86**, 3993 (2001).
[9] X. Sun and K. B. MacAdam, Phys. Rev. A **47**, 3913 (1993).
[10] T. Vogt, M. Viteau, J. Zhao, A. Chotia, D. Comparat, and P. Pillet, Phys. Rev. Lett. **97**, 083003 (2006); T. Vogt, M. Viteau, A. Chotia, J. Zhao, D. Comparat, and P. Pillet, *ibid.* **99**, 073002 (2007).
[11] A. Tauschinsky, C. S. E. van Ditzhuijzen, L. D. Noordam, and H. B. van Linden van den Heuvell, Phys. Rev. A **78**, 063409 (2008).
[12] A. Reinhard, T. Cubel Liebisch, K. C. Younge, P. R. Berman, and G. Raithel, Phys. Rev. Lett. **100**, 123007 (2008); T. Amthor, J. Denskat, C. Giese, N. N. Bezuglov, A. Ekers, L. S. Cederbaum, and M. Weidemüller, Eur. Phys. J. D **53**, 329 (2009); D. Comparat and P. Pillet, J. Opt. Soc. Am. B **27**, A208 (2010).
[13] S. Chao, M. Hayashi, S. Lin, and E. Schlag, J. Phys. B **31**, 2007 (1999).
[14] D. Vrinceanu and M. R. Flannery, Phys. Rev. Lett. **85**, 4880 (2000).
[15] I. Ryabtsev, D. Tretyakov, and I. Beterov, J. Phys. B **36**, 297 (2003).
[16] R. R. Jones and T. F. Gallagher, Phys. Rev. A **38**, 2846 (1988).
[17] M. L. Zimmerman, M. G. Littman, M. M. Kash, and D. Kleppner, Phys. Rev. A **20**, 2251 (1979).
[18] Y. He, J. Phys. B **45**, 015001 (2012).
[19] F. A. Jenkins and H. E. White, *Fundamentals of Optics*, 4th ed. (McGraw–Hill, New York, 2001).
[20] J. Tallant, S. T. Rittenhouse, D. Booth, H. R. Sadeghpour, and J. P. Shaffer, Phys. Rev. Lett. **109**, 173202 (2012).